Spectral Diagnostics of Blue Stars with Winds

J. Puls and R.-P. Kudritzki[1]

Universitätssternwarte München, Scheinerstr. 1, D-81679 München, Germany

A. E. Santolaya-Rey and A. Herrero

Instituto de Astrofisica de Canarias (IAC), La Laguna, Tenerife, Spain

S. P. Owocki

Bartol Research Institute of the University of Delaware, Newark, DE 19716, USA

J. K. McCarthy

Palomar Observatory, California Institute of Technology, Pasadena, CA 91125, USA

Abstract. In this paper, we present recently developed methods to perform routine spectroscopic analyses of blue stars with winds, as well as a number of results obtained by our group lately. In particular, we discuss the presence of *photospheric* Hα emission in late-B and A supergiants with small mass-loss rates and – as an example – describe a first coarse analysis of the B6–8 I object M31 41-4918.

From our analysis of a large sample of Galactic O stars, we have found a discrepancy between observed and theoretically predicted wind-momentum rates. Whereas at large performance numbers the predictions are too low (which is most probably related to the effects of multi-line scattering), at low performance numbers, i.e., in thin winds, they are too high. Part of this problem is attributed to a failure of the Sobolev approximation in the transsonic region.

1. Introduction

One of the present tasks in massive-star physics is the *routine analysis* of their spectra, since, due to both the actual (and long-standing) questions to be answered and to the enormous amount of data now or soon available, reliable parameters for *large samples* of objects are urgently required. Just to point out a few of these problems (which are covered in detail elsewhere in these proceed-

[1]Max-Planck Institut für Astrophysik, Karl-Schwarzschild-Str. 1, D-85740 Garching, Germany

ings), one has to determine abundances and stellar/wind parameters in order to investigate the topics of:

- stellar evolution (now as function of rotation), which requires the determination of He ($Y_{\rm He}$) and CNO abundances as a function of stellar parameters,
- galactic abundance gradients (chemodynamical evolution of galaxies),
- mass loss as a function of (iron-group) metallicity Z,
- tests and improvements of the theory of radiatively-driven winds,
- massive stars as extragalactic standard candles (e.g., by establishing and calibrating the Wind-momentum–Luminosity Relation (WLR)).

With respect to spectral diagnostics, this means that one has to fix in parallel $T_{\rm eff}$, $\log g$, and $Y_{\rm He}$, plus the desired abundances, if the mass-loss rate $\dot{M}$ of the considered object is low or the lines are weak, whereas in cases of significant mass-loss the wind parameters $\dot{M}$, v_∞, $v(r)$, and the stellar radius R_*, have to be determined simultanously with the previous quantities.

Especially in the latter case, extremely fast methods are required since the number of parameters to be varied is large and the profiles themselves – with a variety of shapes – have to be fitted instead of equivalent widths, thus demanding at least a partly interactive approach.

In this paper, we report on progress made in our working group with respect to this objective, and present some newer results as an outcome of these investigations.

2. Stellar and Wind Parameters for O Stars in the Galaxy and the Magellanic Clouds

In a first attempt, we have analyzed a sample of 24 Galactic, 6 LMC, and 8 SMC O stars of different spectral types and luminosity class with respect to their stellar and wind properties (for details, cf. Puls et al. 1996). The basic method of our approach will be sketched in the following.

The stellar parameters $T_{\rm eff}$, $\log g$, and $Y_{\rm He}$ have been taken from a non-LTE analysis using plane-parallel models, mostly from the work by Herrero et al. (1992). Note, however, that in parallel with the mass-loss determination the value for $\log g$ has been corrected both for wind emission in Hγ (if present) and, within a reasonable approximation, for the different atmospheric density structure of winds. Compared to hydrostatic photospheres, this leads to a different (electron) density in the Stark-wing-forming regions if $\dot{M}$ becomes significant (cf. Fig. 3).

The terminal velocities have been obtained from UV resonance lines (observed by IUE, HST, or ORFEUS) by a method comparable to the SEI approach (Lamers et al. 1987), accounting for a *depth dependent* velocity dispersion ('micro-turbulence') and a non-parameterized ionization structure, which is determined in parallel with the line fit (Haser et al. 1994).

Finally, the mass-loss rate (and, where possible, the β exponent of the assumed velocity law) were found by a detailed fit to the Hα line, with a consistent inclusion of the neighbouring He II blend, non-LTE effects, and the Stark-broadened photospheric profile.

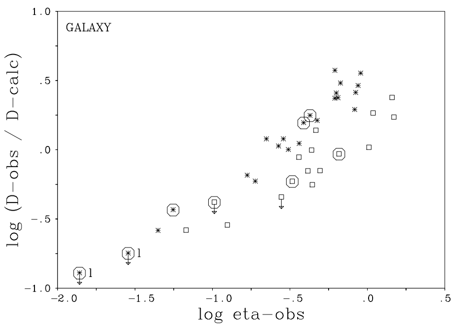

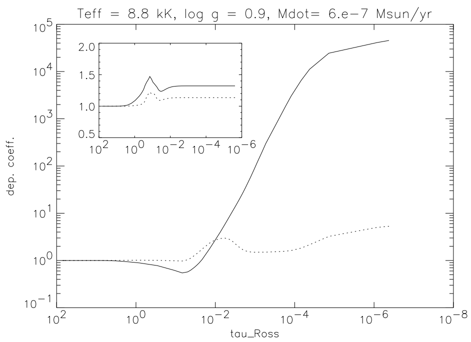

Figure 1. (Left) logarithmic difference of observed wind momentum rate and theoretical prediction as function of wind performance number for Galactic O-stars. Asterisks: $T_{\rm eff} < 40\,000$ K; squares: $T_{\rm eff} \geq 40\,000$ K. Fast rotators are indicated by a circle, and arrows indicate upper limits. (From Puls et al. 1996.)

Figure 2. (Right) Non-LTE departure coefficients for the 2nd (—) and 3rd (...) level of hydrogen, for an A-supergiant model with moderate wind. Shown as insert: corresponding quantities for a typical O4 supergiant.

In order to obtain a fast and interactive line fit, but to avoid the time-consuming calculation of a large number of non-LTE models and departure coefficients, we made use of a grid of 'unified' stellar-atmosphere models (cf. Gabler et al. 1989) available to our group. After investigating the run of the non-LTE departure coeffients of the relevant levels of H I and He II, it turned out that, in the *O-star domain,* these can be parameterized as a simple function of velocity and mean wind density. This parameterization was used in our line-fitting method and enabled the desired interactive procedure. Since in the considered region of the HRD the hydrogen departure coefficients are not too large in any case (cf. the insert of Fig. 2), small inaccuracies in our approximation are insignificant.

The typical Hα fit quality for O stars of different luminosity classes turned out to be very promising (cf. Fig. 17 in Puls et al. 1996). For those objects where the profile is significantly filled in by wind emission, $\dot{M}$ could be fixed to better than $\pm 30\%$, and, if the profiles showed pronounced wind *emission,* we could determine additionally the exponent β of the assumed velocity law from the form of the emission peak. Interestingly, for almost all supergiants we found β-values in the range of 1.0–1.4, in contrast to present theoretical simulations which produce the 'standard' value of radiatively-driven wind theory, $\beta \simeq 0.8$, in almost all cases which are not very close to the Eddington limit.

The derived parameters were used in two ways. First, they constitute the basic data set for establishing the now well-known WLR in the O-star domain (Kudritzki et al. 1995). Second, we performed a comparison between the derived values and the theoretical predictions from the Munich radiation-driven wind code (Pauldrach et al. 1994), which confirmed in part previous results of a similar investigation by Lamers & Leitherer (1993). (For a discussion of this coincidence, which is the result of two effectively compensating inconsistencies, see Puls et al. 1996.)

In Fig. 1, we have plotted the ratio of observed to predicted wind-momentum rate $D = \dot{M} v_\infty$ versus observed wind-performance number $\eta = (\dot{M} v_\infty)/(L/c)$, where L/c is the momentum rate of the stellar radiation field (with L the luminosity).

From this figure, the deficiencies of our present theoretical description are obvious. Whereas at low performance numbers (i.e., thin winds) the predictions yield too large a value for the momentum rate, for wind performances around unity they are too low! Possible reasons for the former discrepancy are discussed in Section 4, while the latter one is most probably related to the fact that the Munich wind code presently neglects the effects of multi-line scattering in the calculation of the radiative acceleration. Test calculations by de Koter et al. (1997) accounting for multi-line scattering explicitly by means of a Monte-Carlo transfer indicate that the situation improves significantly if this additional 'source of momentum' is considered. Further support of this hypothesis is given by the fact that the momentum discrepancy is more pronounced for cooler O stars than for hotter ones (asteriks vs. squares). In the cooler domain, one might expect larger multi-line effects due to the higher incidence of *stratified* ionization zones (which are major ingredients for improving the effectivity of multi-line scattering, cf. Lucy & Abbott, 1993; Schmutz, 1997; Springmann & Puls 1998). Note also that the prototype for most investigations dealing with O-star winds, ζ Pup (the highest-luminosity object indicated as a fast rotator in Fig. 1), does not suffer from any momentum problem, which is in accordance with the findings by Puls (1987) that multi-line effects should be small for this object.

3. A New Tool to Perform Spectral Diagnostics for Blue Stars with Winds

Over the last years, the importance of A- and B-type supergiants as ideal candidates for resolving a number of present scientific questions has been recognized and their impact on current research has considerably increased (e.g., the contributions to this volume by McCarthy et al., Dufton, Massa & Prinja, Monteverde, and Venn et al.). Thus fast analysis methods to obtain consistent stellar *and wind* parameters in this spectral range are in high demand. Unfortunately, the simple method of parameterizing the departure coefficients as outlined above no longer works; mostly because of the increasing optical depth in the Lyman continuum for decreasing temperatures, but also due to wind effects in the resonance lines, the departures from LTE become (very) sensitive to variations of both the stellar and the wind properties, so that a simple and unique parameterization finally becomes more difficult than the calculation of a comprehensive model grid. As an example, in Fig. 2 we compare the rather simple behaviour of the $n = 2, 3$ hydrogen departure coefficients of an O supergiant with the corresponding quantities of an A supergiant. Due to the enormous optical depth in the Lyman continuum and the resonance lines, all radiative rates connecting the hydrogen ground level to the other levels and the continuum are in detailed balance almost throughout the entire atmosphere. In consequence, the second

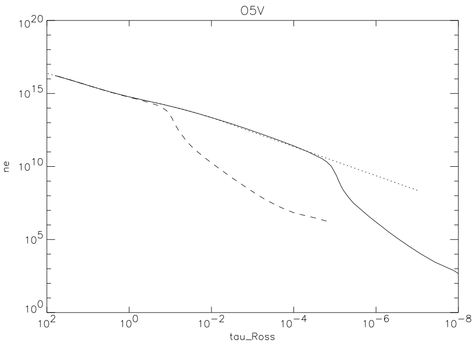

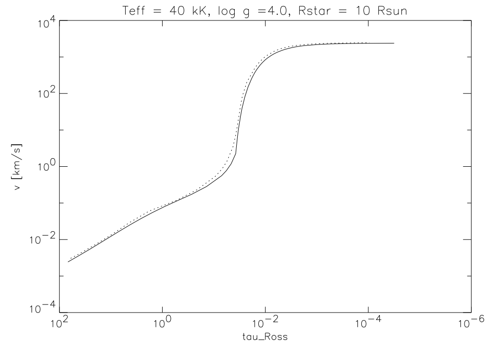

Figure 3. (Left) Comparison of e^--densities: O-star, plane-parallel model atmospere (dotted), and SPH model, with thin (fully drawn) and moderate (dashed) wind (from SPH, 1997).

Figure 4. (Right) Comparison of velocity fields: O star with thin wind, hydrodynamic solution (from Pauldrach et al. 1998, dotted), and SPH model, $\beta = 0.8$ (fully drawn).

level becomes the effective ground state, displaying the typical depopulation in the photosphere and the overpopulation in the wind due to the decreasing ionizing radiation from inside to outside. In consequence, the Hα line changes its character from an optically thin recombination line to an optically thick (quasi-resonance) P-Cygni line, if the spectral type changes from O through B to A.

Additionally, and most importantly with respect to extragalactic work, where the dominant observable population will consist of extreme supergiants or hypergiants, most metal lines will be contaminated by wind effects due to the huge mass loss of these objects (cf. the Fe II/Ti II spectrum of the M33 A supergiant B 324 discussed by McCarthy et al. 1995 and by Venn et al. 1998). Thus, even for abundance determinations – which usually remain rather unaffected by the presence of a wind since only the weakest lines are used for this purpose – mass outflow has to be considered.

In order to meet the present and future challenges of analyzing spectra which are severely affected by stellar outflows, while *also allowing for a consistent treatment in cases of negligible winds,* three of us have developed a new non-LTE atmosphere/line-formation code (henceforth called the 'SPH-code'[2]), which is easy to use, numerically stable, and fast. In the following, we will briefly discuss its principal features (for details, we refer the reader to Santolaya-Rey et al. 1997; SPH).

- The SPH code calculates a 'unified' atmosphere, but for a given mass-loss rate and a predescribed velocity field (usually, but not necessarily, of β-type). It ensures a smooth transition to the 'exact' photospheric stratification, but also accounts for sphericity effects if present. Thus the resulting

[2]Not to be confused with '*S*mooth *P*article *H*ydrodynamics'

structure is consistent with plane-parallel model atmosphereres accounting for the same model atoms at low velocities ($v \ll v_{\rm sound}$) and low values of $\Gamma_{\rm e}$ (the ratio of Thomson acceleration to gravity, cf. Fig. 3). On the other hand, for an input value of $\beta = 0.8$ it relates well to hydrodynamical wind solutions including radiative driving (if similar values for $\dot{M}$ and v_∞ are provided; Fig. 4).

- The SPH code is *flux conserving,* which follows from a simplified calculation of the temperature structure ('non-LTE Hopf function', generalized for spherical symmetry; see also Pauldrach et al. 1998).
- The line transfer is calculated preferentially in the comoving frame, but the code also allows for a Sobolev solution with continuum or a *mixed treatment,* which may turn out to be necessary if very complex ions with thousands of lines (e.g., Fe) are to be included.
- The data management is handled in the philosophy of DETAIL (Butler & Giddings 1985), which guarantees a rather flexible input and the use of a large number of available model atoms. Presently, the code can treat H, He, and Si atoms (Fe is in progress).
- In the formal solution, the appropriate line-broadening functions (Stark, pressure, Lorentz broadening) are used and the redistribution by *incoherent* electron-scattering is accounted for.
- For stellar models with very thin winds and negligible extent, the profiles from non-LTE line-formation codes using plane-parallel atmospheres (e.g., DETAIL/SURFACE) are *perfectly* reproduced.
- Typical computational times (model + non-LTE, all lines in the comoving frame + profiles of strategic lines) on a workstation with 50 MFLOPS are 10 minutes for a pure-hydrogen model, 20 minutes for a H/He model, and 30–40 minutes for a H/He/Si model.
- The 'only' feature which is missing at present is the inclusion of line-blocking/blanketing, which is planned for the next version of the code.

First applications of this code with respect to mass-loss determinations and the calibration of the WLR for A supergiants are discussed in McCarthy et al. (1995, 1997, 1998). In this paper, we want to stress another topic, which is, to our knowledge, prominent only in the domain of luminous A- and late B-type stars, namely the *photospheric* Hα emission (more generally, Balmer-line emission) of these objects when they have low gravity, but not too large a wind density.

Under these conditions, the Hα profile develops a double-peaked emission profile, which is the result of a pure non-LTE effect and in no way related to the presence of a disk or other rotational effects. In Fig. 5, we present a sequence of theoretical Hα profiles for a cool B-supergiant model (very low $\dot{M}$), as the gravity is successively reduced. (The values of $\Gamma_{\rm e}$ vary from 0.6 through 0.75 to 0.85, respectively, for the assumed helium abundance of $Y_{\rm He} = 0.2$.) The displayed effect was first described, operating in LBVs, by Hubeny & Leitherer (1989), and was found to be present, e.g., in the metal-poor M33 A supergiant 117-A (cf. McCarthy et al. 1995). In brief (see also SPH), the line emission results mainly from the *photospheric* depopulation of the second hydrogen level, due to the 'hot' Balmer continuum present in those stars. Thus the resulting

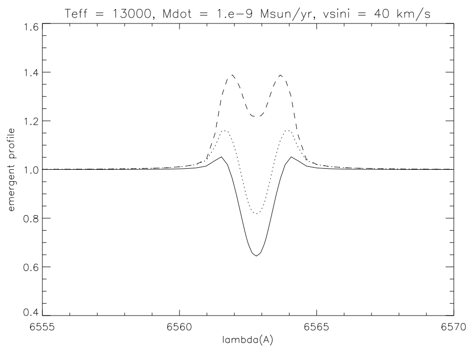

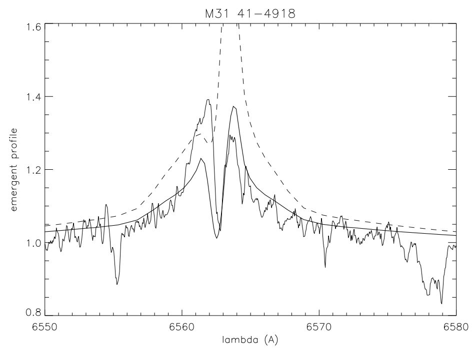

Figure 5. (Left) Photospheric Hα emission of B-supergiant models close to the Eddington limit and with a thin wind. Fully drawn: $\log g = 1.3$; dotted: $\log g = 1.2$; dashed: $\log g = 1.15$ (see text for details).

Figure 6. (Right) Coarse fit to the Hα profile of the M31 B supergiant 41-4918. For observations and parameters, see text. Fits include photospheric and wind emission as well as incoherent electron-scattering. Fully drawn: $\dot{M} = 0.5 \times 10^{-6} M_{\odot}$ yr^{-1}; dashed: $\dot{M} = 1.0 \times 10^{-6} M_{\odot}$ yr^{-1}.

source function is larger than the local Planck function in a certain layer, before, farther out, the line becomes an absorption line again. Note that the effect is only *visible* in those cases when the line is *formed* just in this region, i.e., in cases of thin winds. Now, for decreasing gravity the density also becomes lower, so that the point where the Balmer continuum is formed ($\tau_{\rm Ba} = 1$) will be shifted inside towards higher temperatures, and the effect becomes more pronounced.

One of us (AH) has drawn attention to the Hα profile of the M31 B supergiant 41-4918, a luminous object re-observed with Keck HIRES (cf. McCarthy et al. 1995, 1997, 1998). Since this profile exhibits the discussed double-peak structure, thus pointing to a low wind density *while being luminous,* we have performed a first analysis of this object, both to check the capability of our code and to find additional constraints for the WLR of BA supergiants.

According to a first guess by JMcC and AH, this star has an effective temperature of roughly 12 000 K and a stellar radius (from its V magnitude and the distance to M31) of $\sim 200 R_{\odot}$. The terminal velocity has been guessed from its spectral type (B6–8 I) as 300 km s^{-1}. The radial velocity is 75 km s^{-1}, and $v_{\rm e} \sin i = 40$ km s^{-1}. For these parameters, we have performed a first fit to the Hα profile, allowing only for a variation of $\dot{M}$ and $\log g$.

The result is displayed in Fig. 6. If we include the effects of incoherent electron-scattering, which is important in those cases when the line significantly *injects photons from below the electron-scattering sphere* (i.e., just when the photospheric source function is large), we can fit the profile reasonably well for a gravity of $\log g = 1.1$ and $\dot{M} = 0.5 \times 10^{-6} M_{\odot}$ yr^{-1}. For larger gravities, the emission peaks become significantly less pronounced, whereas for higher $\dot{M}$

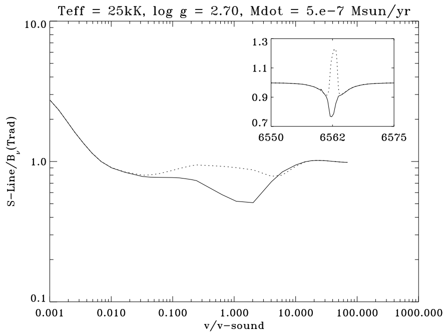

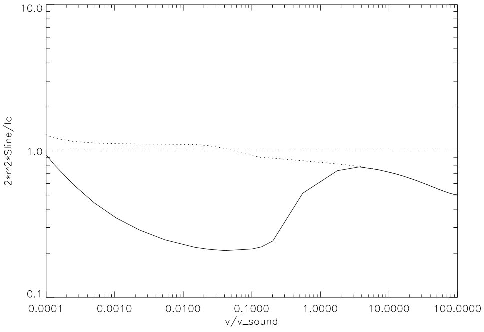

Figure 7. (Left) Hα source function for a B-supergiant model with moderate wind as function of $v/v_{\rm sound}$. Fully drawn, comoving-frame solution; dashed- dotted, Sobolev approximation including continuum processes. Note the marked drop of the source function occuring in the transsonic region for the CMF solution. Also plotted are the emergent profiles for both cases.

Figure 8. (Right) Source function for a strong scattering line in a wind with optically thin continuum: exact solution (CMF, fully drawn) and Sobolev approximation with continuum (dotted). The dashed line gives the asymptotic value in the Sobolev approximation *without* continuum for $r \rightarrow R_*$

they also vanish and the complete profile becomes too strong (cf. the case of $\dot{M} = 1.0 \times 10^{-6} M_\odot$ yr^{-1} in Fig. 6).

A modified wind-momentum rate of $\log(\dot{M} v_\infty R_*^{\frac{1}{2}}) = 28.12$ is implied for a luminosity of $\log(L/L_\odot) = 5.87$. Plotted into the corresponding diagram, this object lies significantly below the WLR for Galactic A and B supergiants (cf. McCarthy et al. 1997, 1998). In order to check whether this can be explained by a (very) low metallicity (note that the M31 A supergiant 41-3654 was found to be iron-deficient; cf. Venn et al. 1998) or whether this result will pose severe problems for our future work, the determination of abundances and a further check of stellar parameters have to be awaited.

4. Line Formation in the Transsonic Region and its Impact on $\dot{M}$ for Thin Winds

One of the lessons we have learnt by calculating theoretical profiles for large model grids is the following: if the line under consideration is formed just in the transsonic region, which is typically the case for Hα in thin or moderate winds, the well-known differences between the Sobolev approximation (even with continuum, cf. Sellmaier et al. 1993) and the exact solution can no longer be neglected. A number of examples were discussed by SPH (1997), and Fig. 7 displays an extreme case. The failure of the Sobolev approximation in the transsonic region (see below) may be also responsible in part for the discrepancies of the theoretically predicted and actually observed wind-momentum rates for thin winds (cf. Fig. 1), and more specifically, for the present overestimate of mass-loss rates if using the standard approach for calculating the line force (cf. Castor, Abbott & Klein 1975 (CAK); Friend & Abbott 1986; Pauldrach, Puls & Kudritzki 1986 (PPK)).

This problem, actually long-standing (Weber 1981, PPK), has come back to our attention during some work related to the evaluation of the line-force instability *including the effects of the disturbed diffuse radiation field* (Owocki & Rybicki 1985; Owocki & Puls 1996), which is part of a present collaboration between SPO and JP. The results of this project will be reported elsewhere, and we want to concentrate here only on the stationary aspect.

The present doctrine of radiation-driven winds is the assertion that the Sobolev approximation can be applied with high precision when calculating radiation forces, as long as only the stationary aspect is considered. This statement was validated by PPK in a careful comparison between the structure arising from using the (modified) CAK approach and the use of radiation forces calculated in the comoving frame. However, as it turned out, these comparisons have been performed only for winds with considerable density!

Fig. 8 compares the run of the source function of a strong scattering line in an optically thin continuum, as calculated by the Sobolev approach and the comoving-frame transfer. Similar to the Hα source function from Fig. 7, but much more pronounced, is the sharp drop of the exact solution in the transsonic region to values much below $0.5 I_c$, where I_c is the irradatiating photospheric intensity[3].

The reason for this drop is primarily given by the enormous change of the velocity field's *curvature* around the sonic point (transition from an exponential to the β-velocity law), which is in stark contrast to the Sobolev assumption of no curvature and which leads to different inward-/outwardly directed escape probabilities, i.e., the usual fore–aft symmetry of scattering line formation is broken[4]. In consequence, the actual source function decreases as $r \rightarrow R_*$. Although the differences between Sobolev and comoving-frame solution seem to be dramatic in the transsonic region, one also has to account for the stabilizing effect due to interactions with the continuum, since the escape probabilites are small at low velocities and the interaction terms (conversion of line into continuum photons) become significant. (We have considered the influence of line collisions as well, but these processes do not change the qualitative essence of our conclusions.) In Fig. 9, we have simulated the same line-formation process as in Fig. 8, but now for different wind strengths, i.e., different continuum optical depths. As it turns out, the decrease of the source function is significant only in cases of thin winds, whereas for moderate and thick winds the continuum terms are sufficient to prevent the source function from becoming considerably depressed.

---

[3] This behaviour may lead to a strong reduction of the line drag effect (Lucy 1984) resulting in much larger growth rates for the line-force instability.

[4] For an extensive discussion of the influence of curvature terms and finite-optical-depth effects, which are additionally important for the details of transsonic line formation, see Sellmaier et al. (1993).

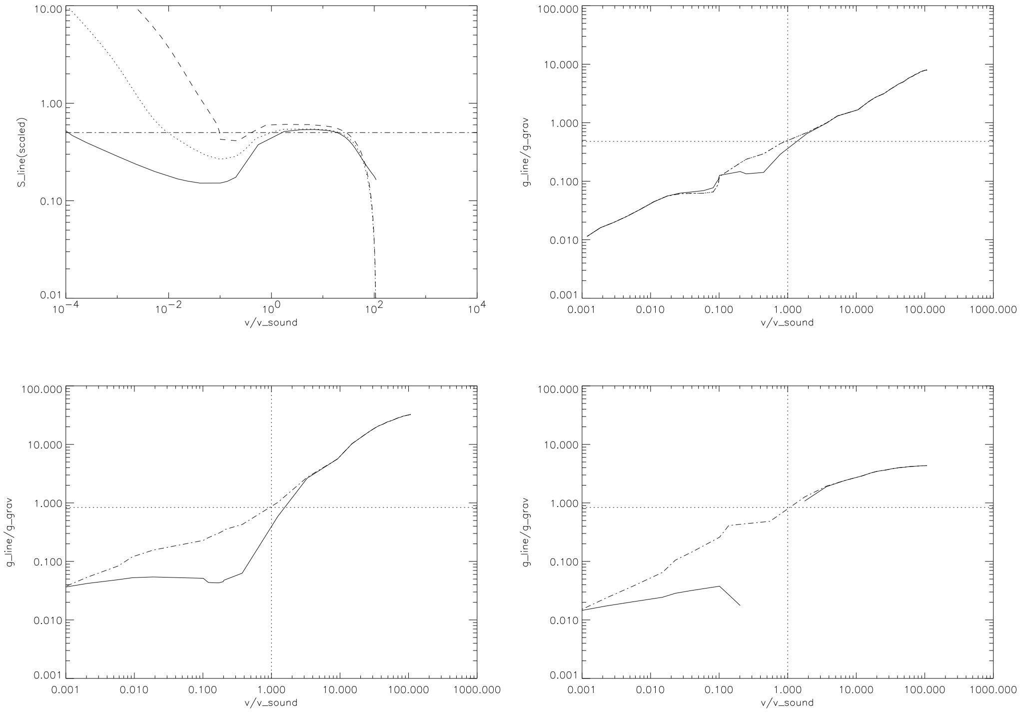

Figure 9. (Upper left) As Fig. 8 (only CMF transfer) for winds with different $\dot{M}$. Thick (dashed), intermediate (dotted), and thin (fully drawn) winds with Rosseland optical depth $\tau_{\rm R} \simeq 0.5$, 0.1, and 0.001, respectively, at the sonic point.

Figure 10. (Upper right, and lower panels) Total line acceleration, $g_{\rm line}$, in units of local gravity for an ensemble of lines (see text) in thick, intermediate, and thin winds; comoving frame (fully drawn) vs. Sobolev approximation (dashed dotted). The horizontal dotted line gives the line acceleration which is required at the sonic point to induce an outflow. Note that in the thin-wind case the exact line force has become negative throughout the transsonic region and is not displayed in this figure.

One might now question the extent to which the extreme behaviour of the source function will influence the line acceleration in thin winds. Under 'normal' conditions, the line force is dominated by the direct term (the diffuse force cancels out due to the symmetric re-emission process), whereas the latter term becomes important in cases of significant source-function gradients (cf. Castor 1974 and Puls & Hummer 1987). Again under normal conditions, this diffuse force is directed outwardly, since the typical source function has a negative gradient with respect to radius. In our case, however, the gradient is positive in a certain range, which induces an *inwardly* directed force component! In order to check the net effect of this process (note that weaker lines are less influenced because of an earlier stabilization by the continuum), we have calculated, for different wind strengths, the total line acceleration arising from a typical *ensemble of lines* (Fig. 10). By summing up the force components of individual lines, we have calculated the total acceleration both in the comoving frame and in the Sobolev approach. The line-strength distribution was assumed according to a force-multiplier parameter $\alpha = 0.6$, and the total number of driving lines was normalized in such a way that the Sobolev force is just sufficient to induce an outflow, i.e., $g_{\,\rm line}(\mathrm{Sob}) = g_{\,\rm grav}(1-\Gamma_{\rm e})$ at the sonic point, neglecting pressure terms. (This method is similar to the procedure discussed by PPK.)

By comparing the Sobolev result with the exact line force, we find only small differences for the thick wind and moderate differences for the intermediate-strength wind (cf. also Fig. 6c in PPK), which would result in similar wind structures in a consistent calculation and which is in agreement with the findings by PPK. For the thin wind, however, the comoving-frame acceleration is no longer sufficient to induce the *predescribed* flow; actually, it has become negative in the complete transsonic region!

Obviously, consistent hydrodynamical calculations have to be performed in order to obtain the final impact of this discrepancy on the resulting wind structure. However, it is tempting to anticipate the following result: if the line force is calculated by the exact approach *and a stationary solution is possible at all,* one may expect a solution with a smaller mass-loss rate, compared to the Sobolev result. This notion is based on the fact that the line acceleration scales (non-linearly) with the inverse density, and, for smaller $\dot{M}$, the acceleration might be sufficient again to overcome the effective gravity.

Finally, we like to stress the following point. The above test calculations have shown that the hydrodynamical simulations of thin winds require the investigation of non-local transfer effects, in order to obtain reliable mass-loss rates. It is also evident, however, that a different line-force stratification will influence the velocity field in the subsonic, as well as the supersonic, wind regions. Especially for the latter, a lower value of $\dot{M}$ means (since the stellar luminosity is still present at its original value) that the acceleration and consequently the terminal velocities should be higher, so that the discussed process can solve only part of the momentum problem, but not the entire one. Of course, there are a number of possibilities that also the theoretically predicted v_∞ (for lower $\dot{M}$) cannot be reached; to quote only two, these are the decoupling of the metal ions from the bulk flow (Springmann & Pauldrach 1992; Babel 1995, 1996) and the influence of near-photospheric line-blocking in thin winds (Puls 1987).

5. Future Work

Fortunately, there is still a lot to be done. Besides the continuation of analyzing large samples of Galactic and extragalactic blue stars and the problems discussed above and elsewhere in these proceedings, we think that the inclusion of line-blocking/blanketing effects in our models has the highest priority. Otherwise, at least the abundance determinations from wind-contaminated metal lines remain doubtful. Although much progress has been obtained over the last years to solve this problem by more or less conventional approaches (e.g., Lanz et al. 1997; Hillier 1997; Hubeny et al. 1998), our philosophy of having *fast* codes at hand requires a different strategy. Most promising is here the method developed by Sellmaier and Pauldrach (Sellmaier 1996; Pauldrach et al. 1998), coupled with approximate non-LTE calculations as developed by Abbott & Lucy (1985) (see also Schmutz 1991, 1997; Lucy & Abbott 1993; Schaerer & Schmutz 1994; and Springmann & Puls 1998 for further improvements and applications).

Acknowledgments. JP gratefully acknowledges a travel grant within the DFG-projects Pu 117/3-1 and Pa 477/1-3.

References

Abbott, D. C., Lucy, L. B., 1985, ApJ, 288, 679

Babel, J., 1995, A&A, 301, 823

Babel, J., 1996, A&A, 309, 867

Butler, K., Giddings, J.R., 1985, in CCP7 Newsletter, ed. C.S. Jeffery (Daresbury Laboratory), no. 9, p. 7

Castor, J. I., 1974, MNRAS, 169, 279

Castor, J. I, Abbott, D. C., Klein, R. I., 1975, ApJ, 195, 157 (CAK)

de Koter, A., Heap, S. R., Hubeny, I., 1997, ApJ, 477, 792

Friend, D. B., Abbott, D. C., 1986, ApJ, 311, 701

Gabler, R., Gabler, A., et al., 1989, A&A, 226, 162

Haser, S. M., Puls, J., Kudritzki, R.-P., 1994, Space Sci. Rev., 66, 187

Herrero, A., Kudritzki, R.-P., et al., 1992, A&A, 261, 209

Hillier, D. J., 1997, ApJ, in press

Hubeny, I., Leitherer, C., 1989, in Physics of Luminous Blue Variables (IAU Coll. 113), eds. K. Davidson, A. F. J. Moffat & H. J. G. L. M. Lamers (Kluwer, Dordrecht), p. 283

Hubeny, I., Heap, S. R., Lanz, T., 1998, in Boulder-Munich II: Properties of Hot, Luminous Stars (ASP Conf. Series, Vol. 131), ed. I. D. Howarth (ASP, San Francisco), p. 108

Kudritzki, R.-P., Lennon, D. J., Puls, J., 1995, in Science with the Very Large Telescope (ESO Astrophysics Symposia), eds. J. R. Walsh & I. J. Danziger (Springer, Heidelberg), p. 246

Lamers, H. J. G. L. M., Cerruti-Sola, M., Perinotto, M., 1987, ApJ, 314, 727

Lamers, H. J. G. L. M., Leitherer, C., 1993, ApJ, 412, 771

Lanz, T., Hubeny, I., Heap, S. R., 1997, ApJ, 485, 843

Lucy, L. B., 1984, ApJ, 284, 351

Lucy, L. B., Abbott, D. C., 1993, ApJ, 405, 738

McCarthy, J. K, Lennon, D. J., et al., 1995, ApJ, 455, L135

McCarthy, J. K., Kudritzki, R.-P., et al., 1997, ApJ, 482, 757

McCarthy., J. K., Venn, K. A., et al., 1998, in Boulder-Munich II: Properties of Hot, Luminous Stars (ASP Conf. Series, Vol. 131), ed. I. D. Howarth (ASP, San Francisco), p. 197

Owocki, S. P., Puls, J., 1996, ApJ, 462, 894

Owocki, S. P., Rybicki, G. B., 1985, ApJ, 299, 265

Pauldrach, A. W. A., Puls, J., Kudritzki, R.-P., 1986, A&A, 164, 86 (PPK)

Pauldrach, A. W. A., Kudritzki, R.-P., et al., 1994, A&A, 283, 525

Pauldrach, A. W. A., Lennon, M., et al., 1998, in Boulder-Munich II: Properties of Hot, Luminous Stars (ASP Conf. Series, Vol. 131), ed. I. D. Howarth (ASP, San Francisco), p. 258

Puls, J., 1987, A&A, 184, 227

Puls, J., Hummer, D. G., 1987, A&A, 191, 87

Puls, J., Kudritzki, R.-P., et al., 1996, A&A, 305, 171

Santolaya-Rey. A. E., Puls, J., Herrero, A., 1997, A&A, 323, 488 (SPH)

Schaerer, D., Schmutz, W., 1994, A&A, 288, 231

Schmutz, W., 1991, in Stellar Atmospheres: Beyond Classical Models (NATO ASI Series C341), eds. L. Crivellari, I. Hubeny & D. G. Hummer (Kluwer, Dordrecht), p. 191

Schmutz, W., 1997, A&A, 321, 268

Sellmaier, F., 1996, Doctoral Thesis, LMU München

Sellmaier, F., Puls, J., Kudritzki, R.-P., Gabler, R., Voels, S. A., 1993, A&A, 273, 533

Springmann, U. W. E., Pauldrach, A. W. A., 1992, A&A, 262, 515

Springmann, U., Puls, J., 1998, in Boulder-Munich II: Properties of Hot, Luminous Stars (ASP Conf. Series, Vol. 131), ed. I. D. Howarth (ASP, San Francisco), p. 286

Venn, K. A., McCarthy, J. K., Lennon, D. J., Kudritzki, R.-P., 1998, in Boulder-Munich II: Properties of Hot, Luminous Stars (ASP Conf. Series, Vol. 131), ed. I. D. Howarth (ASP, San Francisco), p. 177

Weber, S., 1981, ApJ, 243, 954

Discussion

Owocki: One of the things to stress is a corollary to the fact that the source function dips down at the sonic point, which is that it dips below the level necessary for the line-drag effect to suppress the instability there. Therefore, unlike O stars, where the instability really doesn't take hold until you get to maybe a half a stellar radius or so above the star, the prediction for B stars is that the instability will go right down to the basement.